# Angular dependence of the $pp$ elastic scattering spin correlation parameter $A_{00nn}$ between 0.8 and 2.8 GeV. II. Results for higher energies

C. E. Allgower,[1,*] J. Ball,[2,3] M. E. Beddo,[1,†] J. Bystrický,[3] P.-A. Chamouard,[2] M. Combet,[2,3] Ph. Demierre,[4] J.-M. Fontaine,[2,3] D. P. Grosnick,[1,‡] R. Hess,[4,§] Z. Janout,[5,∥] Z. F. Janout,[4,¶] V. A. Kalinnikov,[5] T. E. Kasprzyk,[1] B. A. Khachaturov,[5] R. Kunne,[2,**] F. Lehar,[3] A. de Lesquen,[3] D. Lopiano,[1] I. L. Pisarev,[5] A. A. Popov,[5] A. N. Prokofiev,[6] D. Rapin,[4] J.-L. Sans,[2,††] H. M. Spinka,[1] A. Teglia,[4] Yu. A. Usov,[5] V. V. Vikhrov,[6] B. Vuaridel,[4] and A. A. Zhdanov[6]

[1]*Argonne National Laboratory, HEP Division, 9700 South Cass Avenue, Argonne, Illinois 60439*

[2]*Laboratoire National Saturne, CNRS/IN2P3 and CEA/DSM, CEA/Saclay, 91191 Gif sur Yvette Cedex, France*

[3]*DAPNIA, CEA/Saclay, 91191 Gif sur Yvette Cedex, France*

[4]*DPNC, University of Geneva, 24 quai Ernest-Ansermet, 1211 Geneva 4, Switzerland*

[5]*Laboratory of Nuclear Problems, JINR, RU-141980 Dubna, Moscow Region, Russia*

[6]*Petersburg Nuclear Physics Institute, RU-188350 Gatchina, Russia*

(Received 21 November 2000; published 20 August 2001)

Measurements at 18 beam kinetic energies between 1975 and 2795 MeV and at 795 MeV are reported for the $pp$ elastic scattering spin correlation parameter $A_{00nn}=(N,N;0,0)=C_{NN}=A_{NN}$. The c.m. angular range is typically $60°-100°$. These results are compared to previous data from Saturne II and other accelerators. A search for energy-dependent structure at fixed c.m. angles is performed. Comparisons are made to phase shift analysis and theoretical model predictions of this spin observable.

DOI: 10.1103/PhysRevC.64.034003 PACS number(s): 13.75.Cs, 13.88.+e, 25.40.Cm

## I. INTRODUCTION

This paper presents results from a major experimental program at the Saturne II accelerator in Saclay for $pp$ elastic scattering spin observables up to a kinetic energy of 2800 MeV. These data are from a continuation of the measurements described in Ref. [1] for the polarized beam and polarized target spin correlation parameter $A_{00nn}=(N,N;0,0)=C_{NN}=A_{NN}$. Results were obtained at 19 energies for this paper, and are compared to earlier data from Ref. [1] and other experiments. They significantly increase the $pp$ elastic scattering database, especially at higher energies, and allow a search for rapid energy dependence in this spin observable.

The experiment was performed with a vertically polarized proton beam from Saturne incident on a frozen-spin, vertically polarized proton target during four run periods over a three-year time span. Results for $A_{00nn}$ from the first two run periods (I, II) are presented in Ref. [1]; results from the last two (III, IV) are given here. Each run period lasted 10–14 days, during which measurements were made at several energies. Analyzing power results $A_N=(N,0;0,0)=A_{00n0}=(0,N;0,0)=A_{000n}=P$, and the beam polarization $P_B$ were derived from the same data in Ref. [2] for run periods I and II, and in Ref. [3] for periods III and IV. Analyzing power measurements were performed simultaneously with the polarized beam incident on an unpolarized $CH_2$ target, and these data are published in Ref. [4]. Results for the spin observables $K_{0nn0}=K_{NN}$ and $D_{0n0n}=D_{NN}$ from these same run periods are given in Ref. [5]. For a description of $pp$ elastic scattering spin observables, see Ref. [6].

Roughly half the data sets from run periods III and IV repeat energies from Ref. [1] in order to search for systematic errors and to allow a cross normalization, if necessary. Most of the remaining data sets are above 2.3 GeV, at energies where no previous results exist. A measurement was made at 795 MeV in order to check the absolute target polarization.

The experimental apparatus is described in detail in Refs. [2,3,7–12], including changes to the hardware for the various run periods. A brief description of the polarized beam and target, and of the detectors for the outgoing protons, occurs in Sec. II. The data analysis is described in Sec. III, and the results are presented in Sec. IV. A comparison to phase shift analysis and theoretical model predictions is given in Sec. V.

## II. EXPERIMENTAL APPARATUS

The polarized beam originated in a polarized ion source, and was then accelerated in the Mimas booster ring and the Saturne II accelerator. A number of depolarizing resonances were crossed during acceleration. The beam polarization at the experiment was found from the equality of the beam and target analyzing powers for $pp$ elastic scattering $A_{00n0}=A_{000n}$. This is described in more detail in Ref. [2].

At most energies during run periods III and IV, four beam polarization states were used, designated $0_+$, $-$, $+$, and

*Present address: Indiana University Cyclotron Facility, Bloomington, IN 47408.

†Present address: Data Ventures LLC, Los Alamos, NM 87544.

‡Present address: Department of Physics and Astronomy, Ball State University, Muncie, IN 47306.

§Deceased.

∥Present address: Faculty of Nuclear Sciences and Physical Engineering, Czech Technical University, Břehová 7, 11519 Prague 1, Czech Republic.

¶Present address: Computing Center of the Czech Technical University, Zikova 4, 16635 Prague 6, Czech Republic.

**Present address: Institut de Physique Nucléaire IN2P3, 91400 Orsay, France.

††Present address: Centrale Themis, F-66121 Targasonne, France.

 

$0_-$. The beam pulses normally alternated in the pattern $0_+$, –, +, $0_-$, –, +, $0_+$, –, +, $0_-$, . . . . The relative polarization direction was given by the + and – signs in the labels of the four spin states, with the $0_+$ and $0_-$ states having small polarization magnitudes. Certain beam energy ranges had + corresponding to vertically up, and other ranges to vertically down, caused by the flipping of the beam spin at some strong depolarizing resonances. The four spin states were found to be consistent with being constant with polarization magnitudes

$$P_{0+}:P_-:P_+:P_{0-}=0.072:1.000:1.000:0.072 \qquad (1)$$

as described in Ref. [2], and the special measurements [13] made after these data were collected. These four magnitudes were then multiplied by a different constant at different times as the ion source polarization changed or the accelerator depolarization varied. The typical magnitude for $P_+$ or $P_-$ was $0.6-0.9$.

Three relative beam polarimeters were used to monitor the vertical ($N$-type) and horizontal ($S$-type) transverse components of the beam polarization. These were the SD3 polarimeter [2,3,8] located approximately midway between the beam extraction point from Saturne and the experimental target, the target-region polarimeter [2] situated slightly upstream of the polarized target, and the downstream polarimeter [3] near the beam stop. They monitored the vertical, horizontal, and vertical components of the beam polarization, respectively.

The beam position at the downstream polarimeter was measured at most energies in run periods III and IV by adjusting the positions of all the polarimeter counters and target to maximize the rate of detected events; see Ref. [3]. The incident beam angle was inferred to vary by less than $\pm 3.1$ mrad from energy to energy, except at 795 MeV. Corrections to the data for the incident beam angle were made only at 795 MeV, however.

The polarized proton target used for these experiments is described in Refs. [2,9,10]. The target size was $49(h)\times 40(w)\times 35(l)$ mm$^3$ and it operated in the frozen-spin mode at a temperature as low as 40 mK and a magnetic holding field of 0.33 T. The target material was pentanol-1 in run period III (this was incorrectly reported to be pentanol-3 in Ref. [3]) and pentanol-2 in run period IV. The typical polarization magnitude was $0.65-0.85$ before entering the frozen-spin mode, and the polarization decay time was $\sim 400$ h. The absolute target polarization was found by a comparison of the NMR signals in the polarized state and when the target material was in thermal equilibrium near 1 K. The thermal equilibrium calibrations were performed before and after each run period, and these calibrations agreed with each other within statistical errors.

The detectors for the outgoing particles were designed for a series of nucleon-nucleon ($pp$ and $np$ elastic, and $pp$ and $pn$ quasielastic) scattering experiments over a large and adjustable angular range [2,3,7,11,12]. The scattered and recoil protons in these measurements were detected in coincidence in two ''arms.'' One arm consisted of a magnetic spectrometer, with trigger scintillation counters, four multiwire proportional chambers, a scintillation counter hodoscope, and finally an array of plastic scintillator neutron counters with associated charged-particle veto counters. The other detector arm included trigger scintillation counters, two multiwire proportional chambers, and a scintillation counter hodoscope.

The trigger was a fivefold coincidence between a trigger scintillation counter and a hodoscope counter from each arm, and one or an adjacent pair of neutron counters (used to detect protons). Information from the multiwire proportional chambers, time-to-digital converters and amplitude-to-digital converters were then read out through CAMAC. Scalers were read at the end of every beam spill. The data acquisition system consisted of a Sun Sparc 1 card running VxWorks software and a SparcStation 1+ computer. Many additional details about the apparatus are given in Refs. [2,3,7,11,12]

### III. DATA ANALYSIS

Details of the data analysis are presented in Refs. [2,3], and are summarized in [1]. The analysis was performed partially independently by two groups, with good agreement between the results. Although much of the analysis software was the same, there were some differences. The results of the two analyses were combined, and the final values are presented in this paper. The quoted ''statistical'' errors include a contribution from the difference in values from the two analyses, as an estimate of the uncertainties associated with the different cuts, background subtractions, and other analysis details.

After estimating and subtracting backgrounds, the number of elastic events was normalized to the relative beam intensity from the target-region polarimeter scalers to give the quantities $n_{ij}$. The subscripts $i$ and $j$ refer to the target and beam polarization states, respectively. The $n_{ij}$ are expected to obey the relations

$$\begin{aligned}
n_{+0+}&=C_0N[1+P_{0+}A_{00n0}+P_{T+}A_{000n}+P_{0+}P_{T+}A_{00nn}],\\
n_{+-}&=C_0N[1-P_-A_{00n0}+P_{T+}A_{000n}-P_-P_{T+}A_{00nn}],\\
n_{++}&=C_0N[1+P_+A_{00n0}+P_{T+}A_{000n}+P_+P_{T+}A_{00nn}],\\
n_{+0-}&=C_0N[1-P_{0-}A_{00n0}+P_{T+}A_{000n}-P_{0-}P_{T+}A_{00nn}],\\
n_{-0+}&=N[1+P_{0+}A_{00n0}-P_{T-}A_{000n}-P_{0+}P_{T-}A_{00nn}],\\
n_{--}&=N[1-P_-A_{00n0}-P_{T-}A_{000n}+P_-P_{T-}A_{00nn}],\\
n_{-+}&=N[1+P_+A_{00n0}-P_{T-}A_{000n}-P_+P_{T-}A_{00nn}],\\
n_{-0-}&=N[1-P_{0-}A_{00n0}-P_{T-}A_{000n}+P_{0-}P_{T-}A_{00nn}],
\end{aligned} \qquad (2)$$

where $P_j$ and $P_{Ti}$ are the beam and target polarizations. The $P_{Ti}$ are expected to be positive numbers, and the $P_j$ are expected to be all positive or all negative. These equations allow for slow efficiency drifts on time scales of hours, comparable to the period between target polarization reversals, with the parameter $C_0$. At most energies, $C_0$ was consistent with 1.00, or no change in efficiency.

However, Eqs. (2) assume efficiencies are constant over time periods of seconds, corresponding to beam polarization changes. Special care was taken to search for and eliminate bad beam spills, or scintillation counters or multiwire proportional chamber wires that exhibited rapid efficiency variations. This removal of bad data was required in order to prevent systematic errors in the determination of $A_{000n}$ (target analyzing power), and thus in the derived value of the beam polarization magnitude ($P_+$ or $P_-$); see Refs. [2,3].

## IV. RESULTS

Equations (2) were solved for the spin correlation parameter $A_{00nn}=C_{NN}=A_{NN}$ at each c.m. angle as described in Ref. [2]. The combined results from the two analyses are given in Table I and Figs. 1–4. The quoted statistical uncertainties $\Delta A_{00nn}$ contain a contribution that is half the difference between the values from the two analyses. Relative errors $\sigma_{\mathrm{rel}}$ are also included in Table I. These consist of the uncertainty in the derived beam polarization in quadrature with the estimated uncertainty in the absolute target polarization ($\pm 3.0\%$). The total error on an individual $A_{00nn}$ point is given by

$$(\delta A_{00nn})^2=(\Delta A_{00nn})^2+(A_{00nn}\times\sigma_{\mathrm{rel}})^2. \tag{3}$$

The angular slope $dA_{00nn}/d\theta$ at 90° c.m. is expected to be zero, since this spin correlation parameter is symmetric around 90° due to the Pauli principle. The measured data in the angular range $\theta_{\mathrm{c.m.}}=90°\pm 5°$ were fit with a straight line to determine both the slope and the value of $A_{00nn}$ at 90°. These are given in Figs. 5 and 6, along with results from Ref. [1]. The values of $dA_{00nn}/d\theta$ at 90° are seen to be consistent with zero at all energies, as expected. Note that the $A_{00nn}(90°)$ points are shown with combined statistical and systematic uncertainties $\delta A_{00nn}$, and that the preliminary results in Ref. [14] are superceded by those in Ref. [1].

Figures 1 and 2 contain a comparison of data from this paper and from Ref. [1]. Only statistical uncertainties are shown in these figures. The agreement between the different data sets at each energy is generally quite good, except near 2225 MeV, especially if the systematic errors ($\sigma_{\mathrm{rel}}$) are taken into account. The results from Ref. [1] at 2205, 2215, 2225, and 2235 MeV were all taken within a couple days during run period I, with the proton beam accelerated to 2240 MeV. Degraders were added for the three lower energies, in order to avoid a strong depolarizing resonance in Saturne at 2.2016 GeV. The results in Table I at 2215 and 2235 MeV were obtained in run period III, and at 2225 MeV in run period IV; none of these data used a degrader in the beam. The data from run period I are seen to fall slightly below the new measurements at 2215 MeV, and are somewhat above at 2225 and 2235 MeV. This is exactly the same pattern observed in the $A_N$ data in Ref. [3]. Although careful searches for hardware problems or other systematic errors were performed, none were identified. Based on these facts, it is believed that the beam polarization derived in Ref. [3] for the 2225 MeV data from run period IV was too large. This was probably caused by a statistical fluctuation. The two sets of data at 2225 MeV differ by about three standard deviations ($\sigma_{\mathrm{rel}}$).

Previous measurements are also shown in Figs. 1–3. The Bell *et al.* data [15] at 1967 MeV and the Miller *et al.* results [16] at 2205 MeV from the ZGS agree well with the present data, though the Miller *et al.* values are somewhat larger in magnitude. The Lehar *et al.* data [17] at 2396 and 2696 MeV from Saturne also agree very well with results from this experiment. When quoted systematic uncertainties in normalization are considered, the overall agreement of the various data sets is quite good.

One of the larger contributions to the total systematic error on the $A_{00nn}$ results is the uncertainty in the absolute target polarization. Data were collected at 795 MeV during run period IV to check the absolute target polarization with respect to the better known beam polarization, using the analyzing power and the relation $A_{000n}=A_{00n0}$. Note that very good agreement was found with the LAMPF data in Ref. [3]. An alternate test can be made with $A_{00nn}$ and the precise LAMPF measurements of McNaughton *et al.* [18]; see Fig. 4. (Earlier Saturne data are also shown from Bystrický *et al.* [19].) Again, very good agreement is found. A weighted average of the ratio of the two data sets as a function of $\theta_{\mathrm{c.m.}}$ gives

$$\left\langle \frac{A_{00nn}(\mathrm{Saclay})}{A_{00nn}(\mathrm{LAMPF})} \right\rangle = 0.995\pm 0.014,$$

where only the statistical error is quoted. It is concluded that the Saclay and LAMPF normalizations agree within statistical uncertainties.

A search was performed for rapid energy dependence in $A_{NN}$. Data from Ref. [1] and this paper were averaged over the c.m. angular ranges $65°-75°$ and $75°-85°$, and the results are shown in Fig. 7. In addition, data from Bell *et al.* [15] at 1968 MeV, Miller *et al.* [16] at 2205 MeV, Lehar *et al.* [17] at 1796, 2096, 2396, and 2696 MeV, and Lin *et al.* [20] at 1732, 2300, and 2685 are included. The errors shown include both statistical and systematic uncertainties, and good agreement is evident among all the results presented. The values of $A_{00nn}$ at 90° are also given over a wider energy range in Fig. 6. The 90° c.m. values are approximately constant within statistical errors from about 1.0 to 1.8 GeV, reaching a weakly pronounced maximum in the interval from 1.8 to 2.0 GeV, and dropping by about 0.2 between 2.0 and 2.24 GeV. Then $A_{00nn}(90°)$ remains nearly constant up to 2.7 GeV, followed by a fall of about a factor of 3 to a value near 0.1, where it remains up to a much higher energy [20]. Somewhat similar behavior is observed at 80°, though the behavior becomes less pronounced as the angle decreases. A future article will present further discussion about evidence for possible resonancelike effects in these data.

The $A_{00nn}(90°)$ results can be interpreted in terms of the sum of spin-singlet partial waves as

$$d\sigma/d\Omega(1-A_{00nn})=2I_s\propto\left|\sum_{J\ \mathrm{even}}(\text{spin-singlet})_J\right|^2,$$

TABLE I. Measured values of $A_{00nn}=C_{NN}=A_{NN}$ and the associated statistical errors $\Delta A_{00nn}$. The quantities $\langle \theta_{c.m.} \rangle$ and $-t$ are the central values of the c.m. angle and four-momentum transfer squared for each bin in degrees and $(\mathrm{GeV}/c)^2$, respectively. The fractional systematic uncertainty due to knowledge of the absolute beam and target polarization is $\sigma_{rel}$.

| $\langle \theta_{c.m.} \rangle$ | $-t$ | $A_{00nn}$ | $\Delta A_{00nn}$ |
|---|---|---|---|
| (a) 795 MeV, $\sigma_{rel}=\pm 0.032$ | | | |
| 47.4 | 0.241 | 0.5588 | 0.0276 |
| 48.2 | 0.249 | 0.5677 | 0.0109 |
| 49.2 | 0.258 | 0.5621 | 0.0158 |
| 50.2 | 0.269 | 0.5751 | 0.0108 |
| 51.1 | 0.278 | 0.5736 | 0.0201 |
| 52.1 | 0.288 | 0.5700 | 0.0140 |
| 53.1 | 0.298 | 0.5831 | 0.0285 |
| 54.2 | 0.309 | 0.5859 | 0.0156 |
| 55.1 | 0.320 | 0.5887 | 0.0160 |
| 56.2 | 0.331 | 0.5890 | 0.0256 |
| 57.1 | 0.341 | 0.5967 | 0.0153 |
| 58.1 | 0.352 | 0.5889 | 0.0198 |
| 59.1 | 0.363 | 0.5862 | 0.0162 |
| 60.1 | 0.374 | 0.6008 | 0.0156 |
| 61.1 | 0.385 | 0.6042 | 0.0153 |
| 62.1 | 0.397 | 0.5932 | 0.0106 |
| 63.1 | 0.409 | 0.6039 | 0.0118 |
| 64.1 | 0.420 | 0.5917 | 0.0191 |
| 65.1 | 0.432 | 0.6040 | 0.0106 |
| 66.0 | 0.443 | 0.5945 | 0.0165 |
| 67.1 | 0.455 | 0.6214 | 0.0142 |
| 68.1 | 0.467 | 0.6060 | 0.0137 |
| 69.1 | 0.479 | 0.5980 | 0.0106 |
| 70.1 | 0.491 | 0.6075 | 0.0087 |
| 71.0 | 0.504 | 0.6035 | 0.0143 |
| 72.1 | 0.517 | 0.6030 | 0.0137 |
| 73.1 | 0.529 | 0.6206 | 0.0099 |
| 74.0 | 0.541 | 0.6095 | 0.0144 |
| 75.1 | 0.554 | 0.6080 | 0.0163 |
| 76.0 | 0.566 | 0.6234 | 0.0089 |
| 77.1 | 0.579 | 0.6088 | 0.0164 |
| 78.0 | 0.591 | 0.6184 | 0.0119 |
| 79.0 | 0.604 | 0.6442 | 0.0110 |
| 80.0 | 0.617 | 0.6432 | 0.0153 |
| 81.0 | 0.630 | 0.6145 | 0.0099 |
| 82.0 | 0.642 | 0.6347 | 0.0184 |
| 83.0 | 0.655 | 0.6267 | 0.0162 |
| 84.0 | 0.668 | 0.6474 | 0.0154 |
| 85.0 | 0.681 | 0.6481 | 0.0170 |
| 86.0 | 0.694 | 0.6505 | 0.0136 |
| 87.0 | 0.707 | 0.6520 | 0.0179 |
| 88.0 | 0.720 | 0.6498 | 0.0146 |
| 88.8 | 0.731 | 0.6660 | 0.0248 |
| 89.7 | 0.742 | 0.6502 | 0.0510 |
| (b) 1975 MeV, $\sigma_{rel}=\pm 0.052$ | | | |
| 60.5 | 0.940 | 0.288 | 0.028 |

TABLE I. (*Continued.*)

| $\langle \theta_{c.m.} \rangle$ | $-t$ | $A_{00nn}$ | $\Delta A_{00nn}$ |
|---|---|---|---|
| (b) Continued | | | |
| 62.0 | 0.983 | 0.313 | 0.024 |
| 64.0 | 1.041 | 0.312 | 0.020 |
| 65.9 | 1.097 | 0.328 | 0.020 |
| 68.0 | 1.160 | 0.370 | 0.022 |
| 70.0 | 1.219 | 0.391 | 0.026 |
| 72.0 | 1.280 | 0.400 | 0.024 |
| 74.0 | 1.342 | 0.444 | 0.023 |
| 76.0 | 1.406 | 0.467 | 0.023 |
| 77.9 | 1.466 | 0.484 | 0.024 |
| 80.0 | 1.533 | 0.469 | 0.024 |
| 82.0 | 1.595 | 0.515 | 0.019 |
| 84.0 | 1.659 | 0.540 | 0.029 |
| 86.0 | 1.725 | 0.616 | 0.033 |
| 88.0 | 1.789 | 0.592 | 0.023 |
| 89.9 | 1.851 | 0.582 | 0.027 |
| 92.0 | 1.919 | 0.553 | 0.025 |
| 94.0 | 1.982 | 0.536 | 0.026 |
| 96.0 | 2.046 | 0.587 | 0.028 |
| 98.0 | 2.110 | 0.519 | 0.039 |
| 99.9 | 2.171 | 0.474 | 0.027 |
| 101.2 | 2.213 | 0.229 | 0.195 |
| (c) 2035 MeV (III), $\sigma_{rel}=\pm 0.051$ | | | |
| 60.2 | 0.962 | 0.224 | 0.021 |
| 62.0 | 1.013 | 0.253 | 0.019 |
| 64.0 | 1.073 | 0.284 | 0.021 |
| 65.9 | 1.130 | 0.317 | 0.022 |
| 68.1 | 1.197 | 0.335 | 0.020 |
| 70.0 | 1.256 | 0.358 | 0.020 |
| 72.0 | 1.319 | 0.344 | 0.018 |
| 74.0 | 1.382 | 0.406 | 0.020 |
| 76.0 | 1.448 | 0.467 | 0.018 |
| 78.0 | 1.511 | 0.444 | 0.021 |
| 79.4 | 1.560 | 0.468 | 0.021 |
| 82.0 | 1.644 | 0.476 | 0.019 |
| 84.0 | 1.710 | 0.492 | 0.020 |
| 86.0 | 1.776 | 0.471 | 0.020 |
| 88.0 | 1.844 | 0.491 | 0.020 |
| 90.0 | 1.909 | 0.508 | 0.023 |
| 92.1 | 1.979 | 0.482 | 0.024 |
| 94.0 | 2.043 | 0.490 | 0.020 |
| 96.0 | 2.110 | 0.463 | 0.020 |
| 98.0 | 2.174 | 0.423 | 0.021 |
| 99.9 | 2.239 | 0.441 | 0.030 |
| 101.3 | 2.283 | 0.478 | 0.051 |
| (d) 2035 MeV (IV), $\sigma_{rel}=\pm 0.056$ | | | |
| 60.3 | 0.964 | 0.178 | 0.022 |
| 62.0 | 1.013 | 0.239 | 0.017 |
| 64.0 | 1.073 | 0.276 | 0.017 |
| 66.0 | 1.131 | 0.284 | 0.019 |

TABLE I. (*Continued.*)

| $\langle\theta_{c.m.}\rangle$ | $-t$ | $A_{00nn}$ | $\Delta A_{00nn}$ |
|---|---|---|---|
| (d) Continued | | | |
| 67.5 | 1.179 | 0.296 | 0.030 |
| 72.0 | 1.321 | 0.335 | 0.019 |
| 74.0 | 1.382 | 0.334 | 0.018 |
| 76.0 | 1.448 | 0.413 | 0.018 |
| 78.0 | 1.512 | 0.371 | 0.019 |
| 80.0 | 1.579 | 0.414 | 0.022 |
| 82.0 | 1.643 | 0.456 | 0.018 |
| 84.0 | 1.710 | 0.470 | 0.019 |
| 86.0 | 1.776 | 0.440 | 0.020 |
| 88.0 | 1.843 | 0.463 | 0.027 |
| 90.0 | 1.909 | 0.462 | 0.019 |
| 92.0 | 1.977 | 0.441 | 0.020 |
| 94.0 | 2.042 | 0.455 | 0.026 |
| 96.0 | 2.109 | 0.432 | 0.020 |
| 98.0 | 2.175 | 0.416 | 0.020 |
| 100.0 | 2.240 | 0.399 | 0.021 |
| 101.3 | 2.284 | 0.367 | 0.052 |
| (e) 2115 MeV, $\sigma_{rel}=\pm0.046$ | | | |
| 58.8 | 0.955 | 0.308 | 0.082 |
| 60.1 | 0.995 | 0.232 | 0.020 |
| 62.0 | 1.052 | 0.250 | 0.025 |
| 64.0 | 1.114 | 0.285 | 0.022 |
| 66.0 | 1.176 | 0.260 | 0.023 |
| 68.0 | 1.243 | 0.303 | 0.022 |
| 70.0 | 1.306 | 0.357 | 0.022 |
| 72.0 | 1.371 | 0.374 | 0.019 |
| 74.0 | 1.437 | 0.373 | 0.021 |
| 76.0 | 1.504 | 0.392 | 0.019 |
| 78.0 | 1.571 | 0.387 | 0.023 |
| 80.0 | 1.640 | 0.424 | 0.021 |
| 82.0 | 1.709 | 0.447 | 0.020 |
| 83.9 | 1.775 | 0.446 | 0.021 |
| 88.1 | 1.917 | 0.454 | 0.021 |
| 90.0 | 1.983 | 0.465 | 0.021 |
| 92.0 | 2.054 | 0.472 | 0.028 |
| 94.0 | 2.123 | 0.456 | 0.025 |
| 96.0 | 2.191 | 0.445 | 0.025 |
| 97.9 | 2.259 | 0.457 | 0.023 |
| 99.9 | 2.327 | 0.425 | 0.023 |
| 101.5 | 2.381 | 0.360 | 0.049 |
| (f) 2155 MeV, $\sigma_{rel}=\pm0.039$ | | | |
| 58.7 | 0.973 | 0.220 | 0.050 |
| 60.1 | 1.013 | 0.209 | 0.017 |
| 62.0 | 1.072 | 0.246 | 0.017 |
| 64.0 | 1.136 | 0.281 | 0.016 |
| 66.0 | 1.199 | 0.306 | 0.015 |
| 68.0 | 1.265 | 0.283 | 0.015 |
| 70.0 | 1.330 | 0.361 | 0.015 |
| 72.0 | 1.397 | 0.359 | 0.016 |

TABLE I. (*Continued.*)

| $\langle\theta_{c.m.}\rangle$ | $-t$ | $A_{00nn}$ | $\Delta A_{00nn}$ |
|---|---|---|---|
| (f) Continued | | | |
| 74.0 | 1.465 | 0.367 | 0.015 |
| 76.0 | 1.533 | 0.391 | 0.016 |
| 78.0 | 1.601 | 0.434 | 0.022 |
| 80.5 | 1.688 | 0.433 | 0.016 |
| 82.0 | 1.742 | 0.459 | 0.020 |
| 83.9 | 1.808 | 0.428 | 0.015 |
| 86.0 | 1.881 | 0.415 | 0.023 |
| 88.1 | 1.955 | 0.453 | 0.016 |
| 90.0 | 2.021 | 0.448 | 0.018 |
| 92.0 | 2.092 | 0.419 | 0.015 |
| 94.0 | 2.163 | 0.432 | 0.015 |
| 96.0 | 2.234 | 0.434 | 0.016 |
| 98.0 | 2.302 | 0.385 | 0.023 |
| 99.9 | 2.371 | 0.412 | 0.020 |
| 101.7 | 2.431 | 0.416 | 0.041 |
| (g) 2175 MeV, $\sigma_{rel}=\pm0.041$ | | | |
| 58.7 | 0.982 | 0.253 | 0.040 |
| 60.0 | 1.021 | 0.218 | 0.018 |
| 62.0 | 1.082 | 0.258 | 0.017 |
| 64.0 | 1.146 | 0.257 | 0.018 |
| 66.0 | 1.211 | 0.313 | 0.018 |
| 68.0 | 1.276 | 0.313 | 0.019 |
| 70.0 | 1.343 | 0.306 | 0.020 |
| 72.0 | 1.410 | 0.324 | 0.017 |
| 74.0 | 1.479 | 0.361 | 0.020 |
| 76.0 | 1.547 | 0.338 | 0.019 |
| 78.0 | 1.616 | 0.412 | 0.018 |
| 80.0 | 1.686 | 0.398 | 0.018 |
| 82.0 | 1.758 | 0.406 | 0.021 |
| 84.0 | 1.826 | 0.427 | 0.019 |
| 86.0 | 1.899 | 0.439 | 0.023 |
| 88.1 | 1.972 | 0.446 | 0.021 |
| 90.0 | 2.040 | 0.432 | 0.020 |
| 92.0 | 2.111 | 0.446 | 0.019 |
| 94.0 | 2.183 | 0.430 | 0.020 |
| 96.0 | 2.254 | 0.437 | 0.022 |
| 98.0 | 2.324 | 0.390 | 0.021 |
| 100.0 | 2.394 | 0.380 | 0.019 |
| 101.7 | 2.456 | 0.433 | 0.037 |
| (h) 2215 MeV, $\sigma_{rel}=\pm0.038$ | | | |
| 58.7 | 1.000 | 0.214 | 0.029 |
| 60.0 | 1.040 | 0.228 | 0.015 |
| 62.0 | 1.103 | 0.273 | 0.015 |
| 64.0 | 1.167 | 0.286 | 0.014 |
| 66.5 | 1.250 | 0.271 | 0.015 |
| 68.0 | 1.299 | 0.291 | 0.015 |
| 70.0 | 1.368 | 0.310 | 0.014 |
| 72.0 | 1.436 | 0.316 | 0.016 |
| 74.0 | 1.506 | 0.345 | 0.015 |
| 76.0 | 1.575 | 0.367 | 0.015 |

TABLE I. (*Continued.*)

| $\langle\theta_{c.m.}\rangle$ | $-t$ | $A_{00nn}$ | $\Delta A_{00nn}$ |
|---|---|---|---|
| (h) Continued | | | |
| 78.0 | 1.646 | 0.378 | 0.015 |
| 80.0 | 1.717 | 0.387 | 0.019 |
| 82.1 | 1.791 | 0.379 | 0.017 |
| 84.0 | 1.861 | 0.430 | 0.015 |
| 86.0 | 1.934 | 0.425 | 0.015 |
| 88.0 | 2.006 | 0.424 | 0.015 |
| 90.0 | 2.078 | 0.433 | 0.019 |
| 92.0 | 2.150 | 0.447 | 0.015 |
| 94.0 | 2.223 | 0.420 | 0.016 |
| 96.0 | 2.296 | 0.413 | 0.016 |
| 98.0 | 2.366 | 0.398 | 0.019 |
| 100.0 | 2.438 | 0.405 | 0.016 |
| 101.8 | 2.504 | 0.348 | 0.017 |
| (i) 2225 MeV, $\sigma_{rel}=\pm 0.049$ | | | |
| 58.7 | 1.005 | 0.189 | 0.052 |
| 60.0 | 1.044 | 0.221 | 0.021 |
| 62.0 | 1.107 | 0.188 | 0.021 |
| 64.0 | 1.172 | 0.196 | 0.021 |
| 66.0 | 1.237 | 0.264 | 0.023 |
| 67.9 | 1.303 | 0.250 | 0.025 |
| 70.0 | 1.375 | 0.293 | 0.033 |
| 72.0 | 1.444 | 0.238 | 0.030 |
| 74.0 | 1.514 | 0.279 | 0.025 |
| 76.0 | 1.582 | 0.276 | 0.037 |
| 78.0 | 1.654 | 0.323 | 0.028 |
| 80.0 | 1.725 | 0.342 | 0.023 |
| 82.1 | 1.800 | 0.324 | 0.025 |
| 84.0 | 1.869 | 0.371 | 0.023 |
| 86.0 | 1.942 | 0.329 | 0.036 |
| 88.0 | 2.014 | 0.317 | 0.029 |
| 90.0 | 2.088 | 0.322 | 0.035 |
| 92.0 | 2.161 | 0.350 | 0.029 |
| 94.0 | 2.233 | 0.381 | 0.026 |
| 96.0 | 2.306 | 0.350 | 0.040 |
| 98.0 | 2.378 | 0.347 | 0.025 |
| 100.0 | 2.451 | 0.305 | 0.028 |
| 101.9 | 2.520 | 0.293 | 0.028 |
| 103.2 | 2.563 | 0.466 | 0.115 |
| (j) 2235 MeV, $\sigma_{rel}=\pm 0.043$ | | | |
| 58.8 | 1.010 | 0.258 | 0.038 |
| 60.0 | 1.048 | 0.271 | 0.019 |
| 62.0 | 1.112 | 0.270 | 0.017 |
| 64.0 | 1.177 | 0.267 | 0.020 |
| 66.0 | 1.245 | 0.289 | 0.018 |
| 68.0 | 1.310 | 0.310 | 0.020 |
| 70.0 | 1.380 | 0.344 | 0.018 |
| 72.0 | 1.449 | 0.349 | 0.020 |
| 74.0 | 1.520 | 0.368 | 0.018 |
| 76.0 | 1.589 | 0.386 | 0.022 |
| 78.0 | 1.661 | 0.394 | 0.019 |

TABLE I. (*Continued.*)

| $\langle\theta_{c.m.}\rangle$ | $-t$ | $A_{00nn}$ | $\Delta A_{00nn}$ |
|---|---|---|---|
| (j) Continued | | | |
| 80.0 | 1.733 | 0.413 | 0.020 |
| 82.1 | 1.808 | 0.401 | 0.021 |
| 84.0 | 1.878 | 0.408 | 0.020 |
| 86.0 | 1.951 | 0.383 | 0.019 |
| 88.0 | 2.024 | 0.403 | 0.019 |
| 90.0 | 2.098 | 0.407 | 0.020 |
| 92.0 | 2.169 | 0.417 | 0.20 |
| 94.0 | 2.244 | 0.408 | 0.020 |
| 96.0 | 2.317 | 0.380 | 0.022 |
| 98.0 | 2.388 | 0.397 | 0.027 |
| 100.0 | 2.460 | 0.403 | 0.022 |
| 101.9 | 2.529 | 0.375 | 0.025 |
| 103.2 | 2.575 | 0.398 | 0.144 |
| (k) 2345 MeV, $\sigma_{rel}=\pm 0.048$ | | | |
| 58.0 | 1.035 | 0.200 | 0.074 |
| 60.0 | 1.101 | 0.226 | 0.023 |
| 62.0 | 1.168 | 0.259 | 0.025 |
| 64.0 | 1.235 | 0.240 | 0.027 |
| 66.0 | 1.306 | 0.232 | 0.028 |
| 68.5 | 1.393 | 0.271 | 0.028 |
| 69.8 | 1.442 | 0.250 | 0.038 |
| 72.0 | 1.520 | 0.313 | 0.043 |
| 74.2 | 1.601 | 0.313 | 0.032 |
| 76.0 | 1.667 | 0.345 | 0.026 |
| 78.0 | 1.743 | 0.357 | 0.028 |
| 80.5 | 1.837 | 0.371 | 0.028 |
| 82.0 | 1.894 | 0.363 | 0.028 |
| 84.0 | 1.971 | 0.316 | 0.027 |
| 86.0 | 2.046 | 0.373 | 0.027 |
| 88.0 | 2.123 | 0.388 | 0.038 |
| 90.0 | 2.201 | 0.356 | 0.038 |
| 92.0 | 2.276 | 0.330 | 0.029 |
| 94.0 | 2.354 | 0.328 | 0.032 |
| 96.0 | 2.430 | 0.360 | 0.029 |
| 98.0 | 2.506 | 0.399 | 0.032 |
| 100.0 | 2.583 | 0.332 | 0.029 |
| 102.0 | 2.658 | 0.319 | 0.032 |
| 103.5 | 2.716 | 0.382 | 0.070 |
| (l) 2395 MeV, $\sigma_{rel}=\pm 0.047$ | | | |
| 60.2 | 1.129 | 0.237 | 0.032 |
| 62.0 | 1.192 | 0.239 | 0.032 |
| 64.0 | 1.261 | 0.229 | 0.030 |
| 66.0 | 1.334 | 0.265 | 0.032 |
| 68.0 | 1.405 | 0.282 | 0.033 |
| 70.1 | 1.481 | 0.300 | 0.032 |
| 72.0 | 1.552 | 0.290 | 0.030 |
| 74.0 | 1.628 | 0.274 | 0.031 |
| 76.0 | 1.702 | 0.307 | 0.032 |
| 78.0 | 1.780 | 0.326 | 0.032 |

TABLE I. (*Continued.*)

| $\langle\theta_{c.m.}\rangle$ | $-t$ | $A_{00nn}$ | $\Delta A_{00nn}$ |
|---|---|---|---|
| (l) Continued | | | |
| 80.0 | 1.856 | 0.333 | 0.036 |
| 81.9 | 1.932 | 0.367 | 0.035 |
| 84.0 | 2.012 | 0.311 | 0.034 |
| 86.0 | 2.089 | 0.389 | 0.034 |
| 88.0 | 2.168 | 0.347 | 0.035 |
| 90.0 | 2.248 | 0.355 | 0.033 |
| 92.0 | 2.326 | 0.364 | 0.034 |
| 94.0 | 2.403 | 0.324 | 0.037 |
| 96.0 | 2.482 | 0.389 | 0.035 |
| 98.0 | 2.560 | 0.337 | 0.037 |
| 100.0 | 2.637 | 0.304 | 0.035 |
| 102.0 | 2.714 | 0.394 | 0.045 |
| 103.7 | 2.778 | 0.407 | 0.043 |
| (m) 2445 MeV, $\sigma_{rel}=\pm 0.049$ | | | |
| 59.7 | 1.137 | 0.218 | 0.057 |
| 62.0 | 1.217 | 0.273 | 0.024 |
| 63.9 | 1.287 | 0.302 | 0.024 |
| 66.0 | 1.362 | 0.330 | 0.025 |
| 68.0 | 1.434 | 0.313 | 0.026 |
| 69.9 | 1.504 | 0.340 | 0.030 |
| 72.0 | 1.585 | 0.334 | 0.055 |
| 74.1 | 1.667 | 0.333 | 0.034 |
| 76.0 | 1.738 | 0.352 | 0.029 |
| 78.0 | 1.817 | 0.302 | 0.036 |
| 80.0 | 1.896 | 0.383 | 0.034 |
| 82.0 | 1.973 | 0.352 | 0.029 |
| 84.0 | 2.056 | 0.348 | 0.029 |
| 86.0 | 2.134 | 0.371 | 0.044 |
| 88.0 | 2.213 | 0.346 | 0.033 |
| 90.0 | 2.295 | 0.376 | 0.031 |
| 92.5 | 2.394 | 0.338 | 0.035 |
| 94.0 | 2.455 | 0.394 | 0.030 |
| 96.0 | 2.534 | 0.357 | 0.032 |
| 98.0 | 2.614 | 0.348 | 0.030 |
| 100.0 | 2.692 | 0.338 | 0.030 |
| 102.0 | 2.771 | 0.378 | 0.029 |
| 103.9 | 2.844 | 0.322 | 0.033 |
| (n) 2495 MeV, $\sigma_{rel}=\pm 0.043$ | | | |
| 60.5 | 1.187 | 0.286 | 0.033 |
| 62.0 | 1.242 | 0.273 | 0.025 |
| 64.0 | 1.313 | 0.286 | 0.025 |
| 66.0 | 1.389 | 0.286 | 0.025 |
| 68.0 | 1.464 | 0.320 | 0.024 |
| 70.0 | 1.539 | 0.327 | 0.046 |
| 72.0 | 1.618 | 0.332 | 0.026 |
| 74.0 | 1.696 | 0.362 | 0.026 |
| 76.0 | 1.773 | 0.342 | 0.028 |
| 78.0 | 1.856 | 0.391 | 0.039 |
| 80.0 | 1.935 | 0.375 | 0.028 |

TABLE I. (*Continued.*)

| $\langle\theta_{c.m.}\rangle$ | $-t$ | $A_{00nn}$ | $\Delta A_{00nn}$ |
|---|---|---|---|
| (n) Continued | | | |
| 82.0 | 2.015 | 0.356 | 0.026 |
| 84.1 | 2.099 | 0.342 | 0.031 |
| 86.0 | 2.178 | 0.401 | 0.030 |
| 88.0 | 2.258 | 0.330 | 0.031 |
| 90.0 | 2.342 | 0.328 | 0.036 |
| 92.0 | 2.423 | 0.352 | 0.029 |
| 94.0 | 2.503 | 0.373 | 0.032 |
| 96.1 | 2.588 | 0.421 | 0.028 |
| 98.0 | 2.668 | 0.358 | 0.032 |
| 100.0 | 2.748 | 0.342 | 0.029 |
| 102.0 | 2.828 | 0.328 | 0.028 |
| 103.9 | 2.905 | 0.331 | 0.036 |
| 105.2 | 2.953 | 0.398 | 0.158 |
| (o) 2515 MeV, $\sigma_{rel}=\pm 0.044$ | | | |
| 60.6 | 1.200 | 0.270 | 0.029 |
| 62.0 | 1.252 | 0.221 | 0.022 |
| 64.0 | 1.324 | 0.275 | 0.028 |
| 66.0 | 1.400 | 0.242 | 0.025 |
| 68.0 | 1.475 | 0.292 | 0.023 |
| 69.9 | 1.549 | 0.272 | 0.025 |
| 71.9 | 1.628 | 0.273 | 0.041 |
| 74.0 | 1.710 | 0.259 | 0.039 |
| 76.1 | 1.791 | 0.256 | 0.026 |
| 78.0 | 1.869 | 0.302 | 0.025 |
| 80.0 | 1.950 | 0.313 | 0.026 |
| 82.0 | 2.031 | 0.334 | 0.029 |
| 84.0 | 2.115 | 0.308 | 0.027 |
| 86.0 | 2.195 | 0.292 | 0.030 |
| 88.0 | 2.276 | 0.328 | 0.028 |
| 90.0 | 2.360 | 0.331 | 0.028 |
| 92.0 | 2.442 | 0.324 | 0.032 |
| 94.0 | 2.524 | 0.348 | 0.028 |
| 96.0 | 2.607 | 0.324 | 0.029 |
| 98.0 | 2.689 | 0.348 | 0.029 |
| 100.0 | 2.770 | 0.304 | 0.028 |
| 102.0 | 2.851 | 0.284 | 0.026 |
| 104.0 | 2.929 | 0.282 | 0.031 |
| 105.2 | 2.979 | 0.236 | 0.082 |
| (p) 2565 MeV, $\sigma_{rel}=\pm 0.044$ | | | |
| 60.7 | 1.228 | 0.228 | 0.042 |
| 62.0 | 1.277 | 0.248 | 0.025 |
| 64.0 | 1.350 | 0.270 | 0.025 |
| 66.0 | 1.427 | 0.307 | 0.027 |
| 68.0 | 1.505 | 0.286 | 0.024 |
| 69.9 | 1.580 | 0.273 | 0.027 |
| 72.1 | 1.665 | 0.293 | 0.038 |
| 74.0 | 1.743 | 0.232 | 0.030 |
| 76.0 | 1.823 | 0.306 | 0.030 |
| 78.0 | 1.908 | 0.328 | 0.032 |

TABLE I. (*Continued.*)

| $\langle\theta_{c.m.}\rangle$ | $-t$ | $A_{00nn}$ | $\Delta A_{00nn}$ |
|---|---|---|---|
| (p) Continued | | | |
| 80.0 | 1.989 | 0.293 | 0.026 |
| 82.0 | 2.071 | 0.305 | 0.043 |
| 84.0 | 2.156 | 0.291 | 0.032 |
| 86.0 | 2.239 | 0.308 | 0.029 |
| 88.0 | 2.322 | 0.266 | 0.029 |
| 90.0 | 2.407 | 0.352 | 0.030 |
| 92.0 | 2.490 | 0.322 | 0.041 |
| 94.0 | 2.575 | 0.328 | 0.036 |
| 96.0 | 2.659 | 0.313 | 0.040 |
| 98.1 | 2.744 | 0.317 | 0.037 |
| 100.0 | 2.825 | 0.319 | 0.036 |
| 102.0 | 2.907 | 0.326 | 0.030 |
| 104.0 | 2.990 | 0.301 | 0.034 |
| 105.3 | 3.043 | 0.326 | 0.052 |
| (q) 2575 MeV, $\sigma_{rel}=\pm0.044$ | | | |
| 60.7 | 1.233 | 0.237 | 0.038 |
| 62.0 | 1.281 | 0.284 | 0.024 |
| 64.0 | 1.356 | 0.316 | 0.025 |
| 66.0 | 1.434 | 0.313 | 0.024 |
| 68.0 | 1.511 | 0.270 | 0.025 |
| 69.9 | 1.587 | 0.275 | 0.027 |
| 71.4 | 1.646 | 0.191 | 0.056 |
| 74.5 | 1.771 | 0.314 | 0.064 |
| 76.5 | 1.852 | 0.296 | 0.030 |
| 78.0 | 1.913 | 0.270 | 0.028 |
| 80.0 | 1.997 | 0.254 | 0.028 |
| 82.0 | 2.079 | 0.290 | 0.030 |
| 84.0 | 2.164 | 0.347 | 0.030 |
| 86.0 | 2.247 | 0.361 | 0.028 |
| 88.0 | 2.331 | 0.310 | 0.032 |
| 90.0 | 2.416 | 0.352 | 0.034 |
| 92.0 | 2.501 | 0.360 | 0.031 |
| 94.0 | 2.585 | 0.305 | 0.029 |
| 96.0 | 2.668 | 0.267 | 0.032 |
| 98.0 | 2.753 | 0.335 | 0.032 |
| 100.0 | 2.836 | 0.326 | 0.030 |
| 102.0 | 2.918 | 0.316 | 0.029 |
| 104.0 | 3.000 | 0.272 | 0.031 |
| 105.3 | 3.054 | 0.338 | 0.061 |
| (r) 2595 MeV, $\sigma_{rel}=\pm0.042$ | | | |
| 60.7 | 1.243 | 0.256 | 0.041 |
| 62.0 | 1.291 | 0.263 | 0.018 |
| 64.0 | 1.367 | 0.272 | 0.020 |
| 66.0 | 1.444 | 0.294 | 0.022 |
| 68.0 | 1.522 | 0.250 | 0.020 |
| 69.9 | 1.599 | 0.304 | 0.028 |
| 72.1 | 1.685 | 0.276 | 0.021 |
| 74.0 | 1.763 | 0.286 | 0.021 |
| 76.0 | 1.844 | 0.287 | 0.022 |
| 78.0 | 1.929 | 0.277 | 0.026 |

TABLE I. (*Continued.*)

| $\langle\theta_{c.m.}\rangle$ | $-t$ | $A_{00nn}$ | $\Delta A_{00nn}$ |
|---|---|---|---|
| (r) Continued | | | |
| 80.0 | 2.013 | 0.291 | 0.022 |
| 82.0 | 2.095 | 0.301 | 0.024 |
| 84.0 | 2.180 | 0.309 | 0.023 |
| 86.0 | 2.265 | 0.331 | 0.030 |
| 88.0 | 2.349 | 0.286 | 0.034 |
| 90.0 | 2.434 | 0.303 | 0.033 |
| 92.0 | 2.521 | 0.353 | 0.025 |
| 94.0 | 2.605 | 0.283 | 0.026 |
| 96.0 | 2.689 | 0.329 | 0.024 |
| 98.0 | 2.774 | 0.310 | 0.024 |
| 100.0 | 2.857 | 0.319 | 0.038 |
| 102.0 | 2.941 | 0.296 | 0.025 |
| 104.0 | 3.024 | 0.288 | 0.023 |
| 105.4 | 3.081 | 0.287 | 0.039 |
| (s) 2645 MeV, $\sigma_{rel}=\pm0.043$ | | | |
| 60.7 | 1.268 | 0.115 | 0.126 |
| 62.0 | 1.318 | 0.273 | 0.025 |
| 64.0 | 1.395 | 0.323 | 0.025 |
| 66.0 | 1.472 | 0.343 | 0.027 |
| 68.0 | 1.551 | 0.307 | 0.029 |
| 69.9 | 1.631 | 0.329 | 0.026 |
| 72.1 | 1.719 | 0.310 | 0.036 |
| 74.0 | 1.797 | 0.327 | 0.034 |
| 76.0 | 1.881 | 0.331 | 0.029 |
| 78.0 | 1.964 | 0.290 | 0.028 |
| 80.0 | 2.052 | 0.330 | 0.027 |
| 82.0 | 2.135 | 0.323 | 0.029 |
| 83.9 | 2.220 | 0.336 | 0.030 |
| 86.0 | 2.308 | 0.322 | 0.029 |
| 88.0 | 2.396 | 0.325 | 0.030 |
| 90.0 | 2.482 | 0.383 | 0.030 |
| 92.0 | 2.570 | 0.337 | 0.033 |
| 94.0 | 2.654 | 0.345 | 0.030 |
| 96.0 | 2.740 | 0.338 | 0.031 |
| 98.0 | 2.828 | 0.330 | 0.029 |
| 100.0 | 2.913 | 0.300 | 0.033 |
| 102.0 | 2.997 | 0.321 | 0.039 |
| 104.0 | 3.082 | 0.308 | 0.027 |
| 105.3 | 3.137 | 0.286 | 0.060 |
| (t) 2795 MeV, $\sigma_{rel}=\pm0.066$ | | | |
| 62.9 | 1.428 | 0.226 | 0.057 |
| 65.5 | 1.535 | 0.220 | 0.062 |
| 68.5 | 1.661 | 0.202 | 0.035 |
| 71.4 | 1.786 | 0.224 | 0.046 |
| 74.4 | 1.917 | 0.247 | 0.096 |
| 77.8 | 2.070 | 0.292 | 0.085 |
| 80.5 | 2.189 | 0.301 | 0.039 |
| 83.4 | 2.323 | 0.131 | 0.049 |
| 86.5 | 2.465 | 0.133 | 0.045 |
| 89.4 | 2.596 | 0.124 | 0.049 |

TABLE I. (*Continued.*)

| $\langle\theta_{\mathrm{c.m.}}\rangle$ | $-t$ | $A_{00nn}$ | $\Delta A_{00nn}$ |
|---|---|---|---|
| (t) Continued | | | |
| 92.5 | 2.738 | 0.178 | 0.050 |
| 95.5 | 2.873 | 0.234 | 0.080 |
| 98.5 | 3.011 | 0.247 | 0.047 |
| 101.6 | 3.148 | 0.228 | 0.051 |
| 104.1 | 3.263 | 0.183 | 0.056 |

where $J$ is the total angular momentum. All spin-singlet waves contribute to the sum above. The 90° differential cross section is similarly proportional to the same combination of spin-singlet waves plus the sum of squares of linear combinations of spin-triplet waves ($d\sigma/d\Omega = I_s + I_t$). Thus, the data in Fig. 6 suggest the spin-singlet contribution is an increasing fraction of the differential cross section at 90° c.m. with energy up to about 2.8 GeV, since

$$1 - A_{00nn} = \frac{2I_s}{I_s + I_t}.$$

Note in this energy range, the differential cross section drops smoothly and continuously with increasing energy. Thus, the $A_{00nn}$ data indicate that the spin-triplet cross section at 90° c.m. $I_t$ drops faster with energy than the corresponding spin-singlet cross section $I_s$ up to 2.8 GeV.

Recently, the Saclay-Geneva group performed a direct reconstruction of the *pp* elastic scattering amplitudes and a phase shift analysis [(PSA), Ref. [21]] at four energies, where many other spin observables had been previously measured. Two solutions were found at 2.7 GeV in Ref. [21]. Introducing recent data from these measurements, the PSA solution at 2.7 GeV becomes unique. The PSA predictions agree closely with $A_{00nn}$ from these experiments at all four energies, and they are shown at 2395 and 2695 MeV in Figs. 2 and 3. Also, the Arndt *et al.* energy-dependent PSA was recently extended from 1.6 to 2.5 GeV [22]. Their predictions from solution SP99 at selected energies are given in Figs. 1–3, and the energy dependence of $A_{00nn}(70°)$, $A_{00nn}(80°)$, and $A_{00nn}(90°)$ are shown in Figs. 6 and 7. The PSA predictions reproduce the data reasonably well and agree closely at 2395 MeV. Note that the data from Ref. [1] and this paper are not included in the SP99 data base of Arndt *et al.*, but are in the data base for the Saclay-Geneva

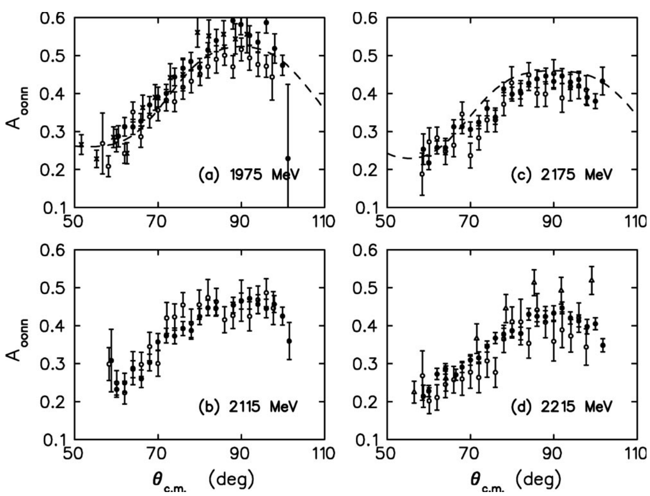


FIG. 1. Experimental results for $A_{00nn} = C_{NN} = A_{NN}$ as a function of c.m. angle at 1975, 2115, 2175, and 2215 MeV. The closed circles are from this paper, the open circles from Ref. [1], the crosses from Bell *et al.* [15], and the open triangles from Miller *et al.* [16]. The dashed lines are from PSA predictions of Arndt *et al.* [22].

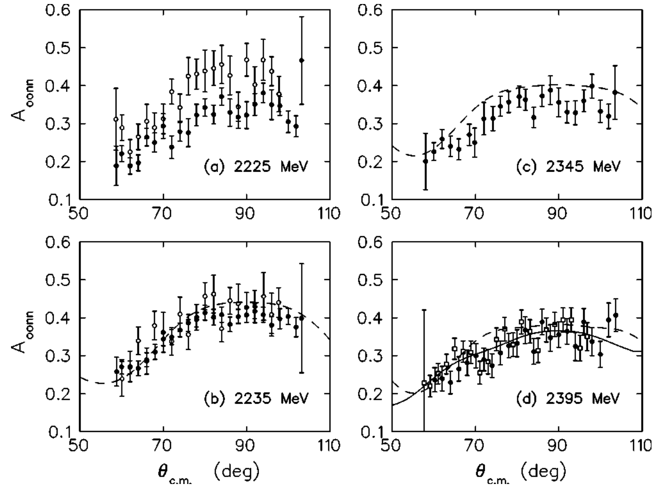


FIG. 2. Experimental results for $A_{00nn} = C_{NN} = A_{NN}$ as a function of c.m. angle at 2225, 2235, 2345, and 2395 MeV. The closed circles are from this paper, the open circles from Ref. [1], and the open squares from Lehar *et al.* [17]. The solid curve is from a PSA prediction of the Saclay-Geneva group [21] and the dashed curves are from Arndt *et al.* [22].

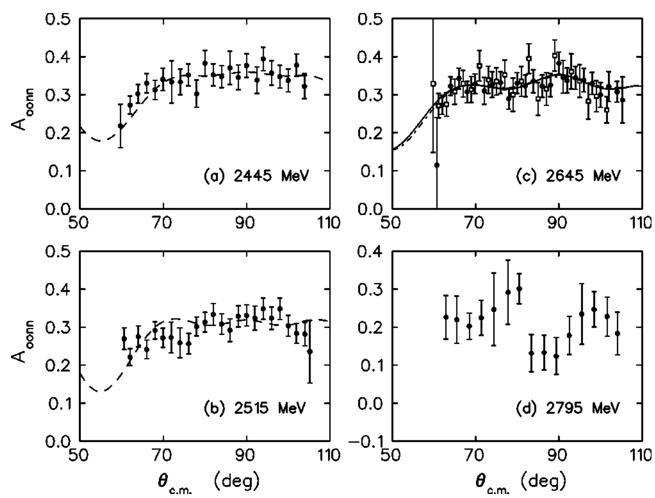


FIG. 3. Experimental results for $A_{00nn} = C_{NN} = A_{NN}$ as a function of c.m. angle at 2445, 2515, 2645, and 2795 MeV. The closed circles are from this paper, and the dashed curve is from a PSA prediction of Arndt *et al.* [22]. The open squares are from Lehar *et al.* [17] at 2696 MeV, and the solid and dot-dashed curves are from PSA predictions of the Saclay-Geneva group [21] also at 2696 MeV.

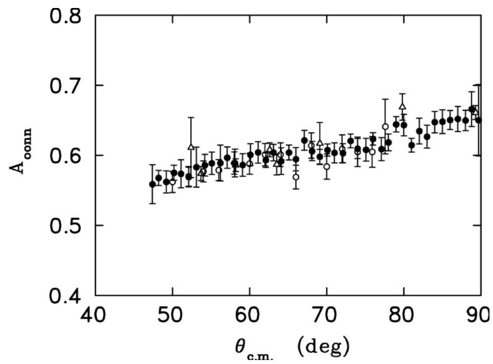


FIG. 4. Experimental results for $A_{00nn}=C_{NN}=A_{NN}$ as a function of c.m. angle at 795 MeV compared to LAMPF data of McNaughton *et al.* [18] (open triangles) and earlier Saturne data of Bystricky *et al.* [19] (open circles). The closed circles are from this paper.

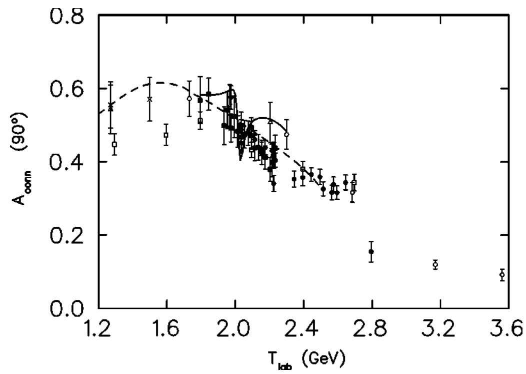


FIG. 6. Experimental values of $A_{00nn}(90°)=C_{NN}(90°)=A_{NN}(90°)$ computed from data between $85°-95°$. The solid circles are from this paper, the solid squares from Ref. [1], the crosses from Bell *et al.* [15], the open triangles from Miller *et al.* [16], the open squares from Lehar *et al.* [17], and the open circles from Lin *et al.* [20]. The dashed curve is from a PSA prediction of Arndt *et al.* [22], and the solid curve is from Lomon [24].

group. The agreement with the PSA predictions is not surprising because of good agreement of the present results with past measurements. (A Japanese group has also recently performed a PSA in this energy region [23].)

A recent prediction of a model by Lomon [24] is also shown in Figs. 6 and 7. This *R*-matrix model (Refs. [25–29]) determines the width and inelasticity of nucleon-nucleon resonances in terms of the algebra of six-quark states and is free of parameters. The masses of the resonances depend on the separation boundary radius, which is fixed to within $\pm 2\%$ by fitting data below $T_{\rm lab}=800$ MeV. This radius forms the boundary between a quark model and a meson exchange description of the nucleon-nucleon interaction. However, the nonresonant background cannot be determined by Lomon's model beyond roughly 1 GeV, and it is taken from the SAID PSA [22]. The predictions in Figs. 6 and 7 correspond to one choice of the relative phase between the lowest mass pp resonance amplitude predicted ($^1S_0$ partial wave, mass $\sim 2.7$ GeV/$c^2$) and the background amplitude containing this partial wave. The energy-dependent structure is similar in shape to the data, with marginal statistical significance. The predictions appear displaced in mass by $\sim 50$–60 MeV (corresponding to a 2% change of separation boundary radius) and in beam energy by roughly 160 MeV, and exhibit about twice the observed magnitude of the structure. Perhaps new measurements from COSY will be able to clarify the experimental situation in the near future.

The data from run periods III and IV, shown in Figs. 1–4, will make a major contribution to the *pp* elastic scattering data base. A total of 20 data sets, at 19 beam kinetic energies, and 477 different points, are included. A careful search for systematic errors, particularly from efficiency changes in the apparatus, was performed. There is good agreement with

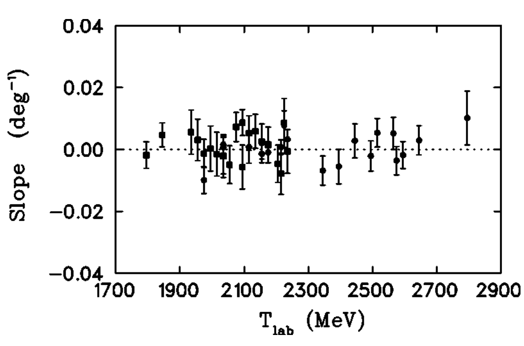


FIG. 5. Plot of the slope $dA_{00nn}/d\theta$ at 90° c.m. as a function of beam kinetic energy. These values were computed from data between $85°-95°$. The solid circles are from this paper and the solid squares from Ref. [1].

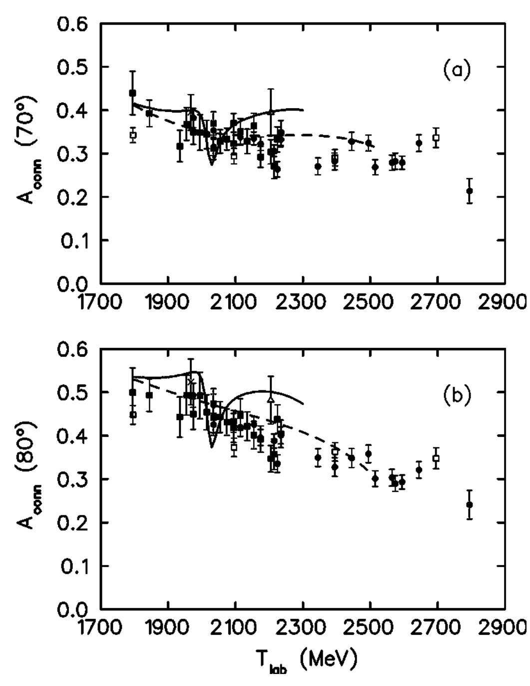


FIG. 7. Experimental results for $A_{00nn}=C_{NN}=A_{NN}$ at (a) 70° and (b) 80° c.m. taken from averages over $65°-75°$ and $75°-85°$. The solid circles are from this paper, the solid squares from Ref. [1], the open squares from Lehar *et al.* [17], the open triangles from Miller *et al.* [16], and the crosses from Bell *et al.* [15]. The dashed curves are from PSA predictions of Arndt *et al.* [22], and the solid curves are from Lomon [24].

data in Ref. [1] when energies were repeated, and with other previous measurements. Many of the data sets are at energies and angles where no previous $A_{00nn}$ results exist, especially at the higher energies.

## ACKNOWLEDGMENTS

We wish to express our thanks to all the operations staff of the Saturne II accelerator for excellent performance of the beams. We are indebted to C. Lechanoine-LeLuc and J. Comfort for their encouraging suggestions, and especially to E. Lomon for providing details and predictions from his cloudy bag model, as well as encouragement for these measurements. This work was supported in part by the U.S. Department of Energy, Division of Nuclear Physics, Contract No. W-31-109-ENG-38, by the Swiss National Science Foundation, and by the Russian Foundation for Fundamental Physics Program 122.03.

[1] C. E. Allgower, J. Ball, L. S. Barabash, P.-Y. Beauvais, M. E. Beddo, N. Borisov, A. Boutefnouchet, J. Bystrický, P.-A. Chamouard, M. Combet, Ph. Demierre, J.-M. Fontaine, V. Ghazikhanian, D. P. Grosnick, R. Hess, Z. Janout, Z. F. Janout, V. A. Kalinnikov, T. E. Kasprzyk, Yu. M. Kazarinov, B. A. Khachaturov, R. Kunne, F. Lehar, A. de Lesquen, D. Lopiano, M. de Mali, V. N. Matafonov, I. L. Pisarev, A. A. Popov, A. N. Prokofiev, D. Rapin, J.-L. Sans, H. M. Spinka, Yu. A. Usov, V. V. Vikhrov, B. Vuaridel, C. A. Whitten, and A. A. Zhdanov, Phys. Rev. C **62**, 064001 (2000).

[2] C. E. Allgower, J. Ball, L. S. Barabash, P.-Y. Beauvais, M. E. Beddo, Y. Bedfer, N. Borisov, A. Boutefnouchet, J. Bystrický, P.-A. Chamouard, M. Combet, Ph. Demierre, J.-M. Fontaine, V. Ghazikhanian, D. P. Grosnick, R. Hess, Z. Janout, Z. F. Janout, V. A. Kalinnikov, T. E. Kasprzyk, Yu. M. Kazarinov, B. A. Khachaturov, R. Kunne, J. M. Lagniel, F. Lehar, J. L. Lemaire, A. de Lesquen, D. Lopiano, M. de Mali, V. N. Matafonov, G. Milleret, I. L. Pisarev, A. A. Popov, A. N. Prokofiev, D. Rapin, J. L. Sans, H. M. Spinka, Yu. A. Usov, V. V. Vikhrov, B. Vuaridel, C. A. Whitten, and A. A. Zhdanov, Phys. Rev. C **60**, 054001 (1999).

[3] C. E. Allgower, J. Ball, M. E. Beddo, J. Bystrický, P.-A. Chamouard, M. Combet, Ph. Demierre, J.-M. Fontaine, D. P. Grosnick, R. Hess, Z. Janout Z. F. Janout, V. A. Kalinnikov, T. E. Kasprzyk, B. A. Khachaturov, R. Kunne, F. Lehar, A. de Lesquen, D. Lopiano, M. de Mali, V. N. Matafonov, I. L. Pisarev, A. A. Popov, A. N. Prokofiev, D. Rapin, J.-L. Sans, H. M. Spinka, A. Teglia, Yu. A. Usov, V. V. Vikharov, B. Vuaridel, and A. A. Zhdanov, Phys. Rev. C **60**, 054002 (1999).

[4] C. E. Allgower, J. Ball, M. Beddo, Y. Bedfer, A. Boutefnouchet, J. Bystricky, P.-A. Chamouard, Ph. Demierre, J.-M. Fontaine, V. Ghazikhanian, D. Grosnick, R. Hess, Z. Janout, Z. F. Janout, V. A. Kalinnikov, T. E. Kasprzyk, B. A. Khachaturov, R. Kunne, F. Lehar, A. de Lesquen, D. Lopiano, V. N. Matafonov, I. L. Pisarev, A. A. Popov, A. N. Prokofiev, D. Rapin, J.-L. Sans, H. M. Spinka, A. Teglia, Yu. A. Usov, V. V. Vikhrov, B. Vuaridel, C. A. Whitten, and A. A. Zhdanov, Nucl. Phys. **A637**, 231 (1998).

[5] C. E. Allgower, J. Ball, L. S. Barabash, M. Beddo, Y. Bedfer, A. Boutefnouchet, J. Bystrický, P.-A. Chamouard, Ph. Demierre, J.-M. Fontaine, V. Ghazikhanian, D. Grosnick, R. Hess, Z. Janout, Z. F. Janout, V. A. Kalinnikov, T. E. Kasprzyk, Yu. M. Kazarinov, B. A. Khachaturov, R. Kunne, C. Lechanoine-LeLuc, F. Lehar, A. de Lesquen, D. Lopiano, M. de Mali, V. N. Matafonov, I. L. Pisarev, A. A. Popov, A. N. Prokofiev, D. Rapin, J.-L. Sans, H. M. Spinka, Yu. A. Usov, V. V. Vikhrov, B. Vuaridel, C. A. Whitten, and A. A. Zhdanov, Eur. Phys. J. C **5**, 453 (1998).

[6] J. Bystrický, F. Lehar, and P. Winternitz, J. Phys. (Paris) **39**, 1 (1978).

[7] C. E. Allgower, Ph.D. thesis, Arizona State University, 1997.

[8] J. Bystrický, J. Derégel, F. Lehar, A. de Lesquen, L. van Rossum, J. M. Fontaine, F. Perrot, C. A. Whitten, T. Hasegawa, C. R. Newsom, W. R. Leo, Y. Onel, S. Dalla Torre-Colautti, A. Penzo, H. Azaiez, and A. Michalowicz, Nucl. Instrum. Methods Phys. Res. A **239**, 131 (1985).

[9] R. Bernard, P. Chaumette, P. Chesny, J. Derégel, R. Duthil, J. Fabre, C. Lesmond, G. Seité, J. Ball, T. I. Niinikoski, and M. Rieubland, Nucl. Instrum. Methods Phys. Res. A **249**, 176 (1986).

[10] J. Ball, M. Combet, J.-L. Sans, B. Benda, P. Chaumette, J. Derégel, G. Durand, A. P. Dzyubak, C. Gaudron, F. Lehar, A. de Lesquen, T. E. Kasprzyk, Z. Janout, B. A. Khachaturov, V. N. Matafonov, and Yu. A. Usov, Nucl. Instrum. Methods Phys. Res. A **381**, 4 (1996).

[11] M. Arignon, J. Bystrický, J. Derégel, F. Lehar, A. de Lesquen, F. Petit, L. van Rossum, J. M. Fontaine, F. Perrot, J. Ball, and C. D. Lac, Nucl. Instrum. Methods Phys. Res. A **262**, 207 (1987).

[12] J. Ball, Ph. Chesny, M. Combet, J. M. Fontaine, R. Kunne, J. L. Sans, J. Bystrický, C. D. Lac, D. Legrand, F. Lehar, A. de Lesquen, M. de Mali, F. Perrot-Kunne, L. van Rossum, P. Bach, Ph. Demierre, G. Gaillard, R. Hess, Z. F. Janout, D. Rapin, Ph. Sormani, B. Vuaridel, J. P. Goudour, R. Binz, A. Klett, E. Rössle, H. Schmitt, L. S. Barabash, Z. Janout, V. A. Kalinnikov, Yu. M. Kazarinov, B. A. Khachaturov, V. N. Matafonov, I. L. Pisarev, A. A. Popov, Yu. A. Usov, M. Beddo, D. Grosnick, T. Kasprzyk, D. Lopiano, and H. Spinka, Nucl. Instrum. Methods Phys. Res. A **327**, 308 (1993).

[13] C. E. Allgower, J. Arvieux, P. Ausset, J. Ball, P.-Y. Beauvais, Y. Bedfer, J. Bystrický, P.-A. Chamouard, P. Demierre, J.-M. Fontaine, Z. Janout, V. A. Kalinnikov, T. E. Kasprzyk, B. A. Khachaturov, R. Kunne, J.-M. Lagniel, F. Lehar, A. de Lesquen, A. A. Popov, A. N. Prokofiev, D. Rapin, J.-L. Sans, H. M. Spinka, A. Teglia, V. V. Vikhrov, B. Vuaridel, and A. A. Zhdanov, Nucl. Instrum. Methods Phys. Res. A **399**, 171 (1997).

[14] J. Ball, P. A. Chamouard, M. Combet, J. M. Fontaine, R. Kunne, J. M. Lagniel, J. L. Lemaire, G. Milleret, J. L. Sans, J. Bystrický, F. Lehar, A. de Lesquen, M. de Mali, Ph. Demierre, R. Hess, Z. F. Janout, E. L. Lomon, D. Rapin, B. Vuaridel, L. S. Barabash, Z. Janout, V. A. Kalinnikov, Yu. M. Kazarinov, B. A. Khachaturov, V. N. Matafonov, I. L. Pisarev, A. A. Popov,

Yu. A. Usov, M. Beddo, D. Grosnick, T. Kasprzyk, D. Lopiano, H. Spinka, A. Boutefnouchet, V. Ghazikhanian, and C. A. Whitten, Phys. Lett. B **320**, 206 (1994).
[15] D. A. Bell, J. A. Buchanan, M. M. Calkin, J. M. Clement, W. H. Dragoset, M. Furić, K. A. Johns, J. D. Lesikar, H. E. Miettinen, T. A. Mulera, G. S. Mutchler, G. C. Phillips, J. B. Roberts, and S. E. Turpin, Phys. Lett. **94B**, 310 (1980).
[16] D. Miller, C. Wilson, R. Giese, D. Hill, K. Nield, P. Rynes, B. Sandler, and A. Yokosawa, Phys. Rev. D **16**, 2016 (1977).
[17] F. Lehar, A. de Lesquen, J. P. Meyer, L. van Rossum, P. Chaumette, J. Derégel, J. Fabre, J.-M. Fontaine, F. Perrot, J. Ball, C. D. Lac, A. Michalowicz, Y. Onel, D. Adams, J. Bystrický, V. Ghazikhanian, C. A. Whitten, and A. Penzo, Nucl. Phys. **B294**, 1013 (1987).
[18] M. W. McNaughton, H. W. Baer, P. R. Bevington, F. H. Cverna, H. B. Willard, E. Winkelmann, E. P. Chamberlin, J. J. Jarmer, N. S. P. King, J. E. Simmons, M. A. Schardt, and H. Willmes, Phys. Rev. C **23**, 838 (1981).
[19] J. Bystrický, P. Chaumette, J. Deregel, J. Fabre, F. Lehar, A. de Lesquen, L. van Rossum, J. M. Fontaine, J. Gosset, F. Perrot, C. A. Whitten, J. Ball, Ph. Chesny, C. R. Newsom, J. Yonnet, T. Niinikoski, M. Rieubland, A. Michalowicz, and S. Dalla Torre-Colautti, Nucl. Phys. **B262**, 727 (1985).
[20] A. Lin, J. R. O'Fallon, L. G. Ratner, P. F. Schultz, K. Abe, D. G. Crabb, R. C. Fernow, A. D. Krisch, A. J. Salthouse, B. Sandler, and K. M. Terwilliger, Phys. Lett. **74B**, 273 (1978).
[21] J. Bystrický, C. Lechanoine-LeLuc, and F. Lehar, Eur. Phys. J. C **4**, 607 (1998).
[22] R. A. Arndt, C. H. Oh, I. I. Strakovsky, R. L. Workman, and F. Dohrmann, Phys. Rev. C **56**, 3005 (1997), and SAID solution SP99.
[23] M. Matsuda, J. Nagata, H. Yoshino, K. Harada, and S. Ohara, Prog. Theor. Phys. **93**, 1059 (1995).
[24] E. L. Lomon (private communication).
[25] E. L. Lomon, J. Phys. (Paris), Colloq. **46**, C2-329 (1985).
[26] P. LaFrance and E. L. Lomon, Phys. Rev. D **34**, 1341 (1986).
[27] P. Gonzalez, P. LaFrance, and E. L. Lomon, Phys. Rev. D **35**, 2142 (1987).
[28] E. L. Lomon, in *Eighth International Symposium on High Energy Spin Physics*, edited by Kenneth J. Heller, AIP Conf. Proc. No. 187 (AIP, New York, 1989), Vol. I, p. 630.
[29] E. L. Lomon, J. Phys. (Paris), Colloq. **51**, C6-363 (1990).